

OmniBind: Teach to Build Unequal-Scale Modality Interaction for Omni-Bind of All

Yuanhuiyi Lyu¹ Xu Zheng¹ Dahun Kim³ Lin Wang^{1,2*}

¹ VLIS LAB, AI Thrust, HKUST(GZ) ²Dept. of CSE, HKUST ³ Google DeepMind
 yuanhuiyilv@hkust-gz.edu.cn, zhengxu128@gmail.com, mcahnny@google.com, linwang@ust.hk

Project Page: <https://vlislab22.github.io/OmniBind/>

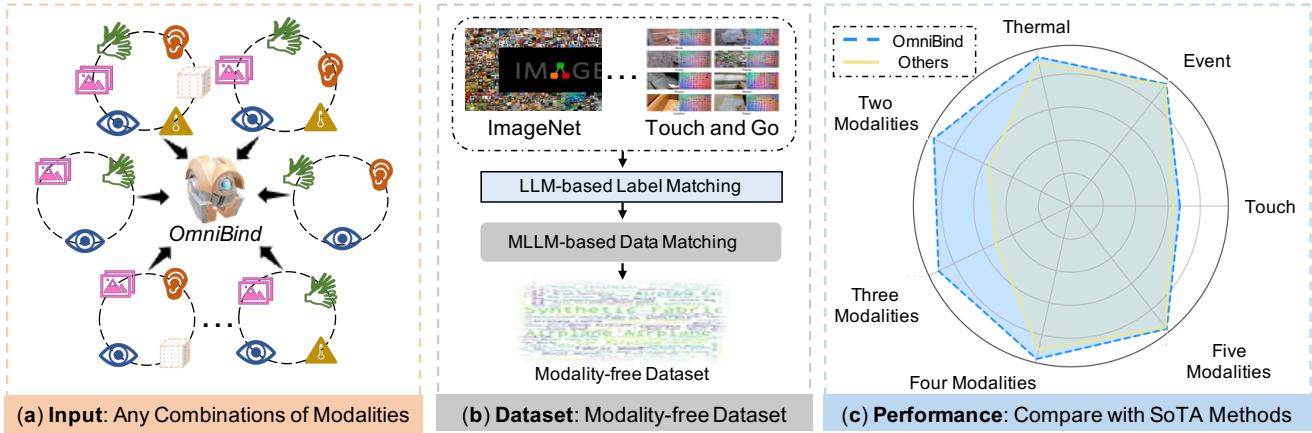


Figure 1. The proposed OmniBind: a novel two-stage learning framework that can achieve any modality combinations and interaction. (a): The ability that accepts input of any modality combinations. (b): The performance of our OmniBind. (c): Modality-free dataset.

Abstract

Research on multi-modal learning dominantly aligns the modalities in a unified space at training, and only a single one is taken for prediction at inference. However, for a real machine, e.g., a robot, sensors could be added or removed at any time. Thus, it is crucial to enable the machine to tackle the mismatch and unequal-scale (or data-scale imbalance) problems of modality combinations between training and inference. In this paper, we tackle these problems from a new perspective: "Modalities Help Modalities". Intuitively, we present **OmniBind**, a novel two-stage learning framework that can achieve any modality combinations and interaction. It involves teaching data-constrained, a.k.a., student, modalities (e.g., touch and thermal) to be aligned with the well-trained data-abundant, a.k.a., teacher, modalities (e.g., image and text). This subtly enables the adaptive fusion of any modalities to build a unified representation space for any combinations. Specifically, we propose **Cross-modal Alignment Distillation (CAD)** to address the

unequal-scale problem between student and teacher modalities and effectively align student modalities into the teacher modalities' representation space in stage one. We then propose an **Adaptive Fusion (AF)** module to fuse any modality combinations and learn a unified representation space in stage two. To address the mismatch problem, we aggregate existing datasets and combine samples from different modalities by the same semantics. This way, we build the **first** dataset for training and evaluation that consists of teacher (image, text) and student (touch, thermal, event, point cloud, audio) modalities and enables omni-bind for any of them, e.g., (image, touch, and event). Extensive experiments show performance gains over prior arts by an average of **4.05%** on the arbitrary modality combination setting. It also achieves the state-of-the-art performance for a single modality, e.g., touch, with **4.34%** gain.

1. Introduction

Humans are naturally equipped with multiple sensing modalities [39, 41], such as vision, audio, and touch,

*Corresponding author.

to understand and perceive the world around us. This has inspired many recent research endeavors for multi-modal foundational models, which can be divided into two categories: 1) multi-encoder-based and 2) universal-transformer-based methods. The first line of methods utilizes a specific modality, *e.g.*, image [14, 15, 64] or language [37, 82], as the alignment center for aligning all modalities to the centric modality. The universal transformer methods [28, 74, 75] utilize a unified transformer for all modalities via modality-specific tokenizers and prompts.

However, in a real-world machine, such as a robot designed to imitate human perception, the configuration of sensors is not static. Sensors may be added, removed, or replaced at any time [23, 68] due to various factors such as environmental conditions, specific task requirements, or technological failures [22, 62]. Thus there exists a mismatch between training and inference if all modalities are used for training and any combinations of these modalities are expected to be achieved during inference. Besides, there is still a significant data-scale imbalance between different modalities. For example, the large gap in data-scale between image modality (*i.e.*, 400 million image data samples) and touch modality (*i.e.*, 12 k data samples).

Therefore, it is essential to equip the machine with the capability to address the mismatch and data-scale imbalance problems of modality combinations between training and inference stages. As depicted in Fig. 1 (a), a machine should possess the capability to integrate any modality combinations at any time, such as image, audio, and point cloud, to achieve robust and reliable scene perception. This flexibility would enable the machine to adapt to different sensor configurations and continue to perform accurately.

In light of this, we introduce **OmniBind**, a two-stage multi-modal learning framework for interacting with any modalities and learning a unified representation space for any modality combinations. The core insight of OmniBind is “*Modalities Help Modalities*,”. It involves teaching data-constrained, *a.k.a.*, *student*, modalities (*e.g.*, touch and thermal) to be aligned with well-trained data-abundant, *a.k.a.*, *teacher*, modalities (*e.g.*, image and texts). This subtly enables the adaptive fusion of any modalities to build a unified representation space for any combinations.

To make this possible, we first introduce the **Cross-modal Alignment Distillation (CAD)** (Sec. 3.2) to tackle the data-scale imbalance problems. It effectively aligns student modalities to the teacher modalities’ representation space at two aspects, *i.e.*, the self-correspondence within each modality and the cross-correspondence between teacher and student modalities. We then propose an **Adaptive Fusion (AF)** module (Sec. 3.3) designed to integrate multi-modal representations from any modality combinations. It facilitates the learning of a unified representation space and consistently demonstrates robust perfor-

mance across diverse modality combinations.

To address the mismatch problem and train our OmniBind, we introduce a modality-free dataset (Sec. 3.4), the first dataset that consists of seven modalities and enables omni-bind for any of them, *e.g.*, (image, touch, and event). As shown in Fig. 1 (b), for aggregating this dataset, we combine the data from different modalities via two-level matching: label-level and sample-level matching.

We evaluate our OmniBind on 1) arbitrary modality combination setting and 2) single modality setting. As shown in Fig. 1 (c), our OmniBind achieves any modality combinations, including combinations of 2-5 modalities. OmniBind shows the remarkable performance of a **4.05%** gain on the arbitrary modality combination setting and also achieves state-of-the-art performance for a single modality, such as a notable **4.34%** gain for the touch modality.

2. Related Work

Multi-modal Foundational Models. Existing vision-language models (VLMs) [6, 11, 29, 30, 40, 46, 54, 70, 78] demonstrate strong performance in aligning language and image modalities into a shared representation space. Subsequent works extend these models to include additional modalities, *e.g.*, audio [17, 38, 55], point cloud [4, 21, 72, 83], and video [8, 32, 35]. Inspired by these VLMs, recent works attempt to build a unified representation space for more than three modalities. Generally, these methods can be divided into two categories: 1) multi-encoder-based and 2) universal transformer-based methods. For the first line of methods, ImageBind [18] is a seminal approach that binds all modalities with the image and builds an image-centric representation space. It has been extended to diverse sensing modalities, such as point cloud [15] and touch [64]. More recently, LanguageBind [82] and UniBind [37] emphasize a language-centric idea and foster the modality-agnostic representation across seven modalities. The universal transformer-based methods [28, 74, 75] utilize a unified transformer for all modalities via modality-specific tokenizers and prompts. However, these methods ignore the mismatch and the unequal-scale (data-scale imbalance) problems among modalities between training and inference. To tackle these problems, our key idea is “modalities help modalities”. Intuitively, we propose the CAD to teach the data-constrained modalities to be aligned with the well-trained data-abundant modalities. Then, the AF module is designed to build a unified representation space for any modality combinations.

Modality Fusion. Many works attempt to fuse multiple modalities to obtain multi-source information [10, 49]. Initial works focus on two-modality fusion, *e.g.*, vision-language [1, 2, 34, 66, 81] or RGB-Depth [59, 76], which amalgamate complementary features from both. However, these methods often experience significant performance

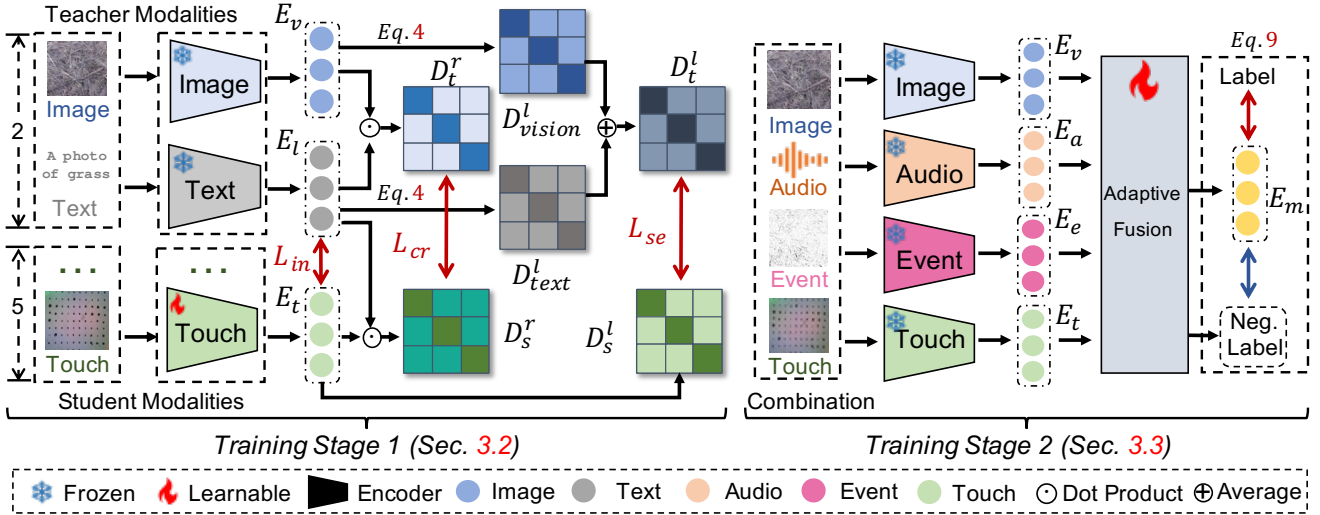


Figure 2. **The overall framework of OmniBind.** We propose a two-stage training approach. *Training stage I:* Aligning the student modalities via CAD module; *Training stage II:* Learning the unified representation space for any modality combination via AF module.

drops when a modality is absent [33, 69, 71, 75]. More recent works explore the fusion of more than three modalities [36, 50, 56], typically using a specific primary modality as a bridge for combining them. Nonetheless, they struggle to handle any modality combinations flexibly during the inference [75]. To address this, we propose the AF module to fuse the multi-modal embeddings and learn a unified representation space for any modality combinations.

Knowledge Distillation aims to transfer the knowledge from a teacher model to student model [20, 52]. Most KD methods focus within a single modality, distilling logits [60, 67], features [19, 47] and relations [44, 63, 79] between models. For the cross-modal KD, the correspondence is widely applied to transfer the knowledge [16, 31, 51, 77]. In our OmniBind, we introduce the CAD module to align the teacher and student models in modalities with unequal-scale (imbalance) data samples by distilling the intra- and cross-modal correspondence.

Multi-modal Datasets serve as the foundation for multi-modal learning. Initially, these datasets only consist of visual data and their corresponding categories [9, 24, 45, 57], which limit their scalability and diversity. To address this issue, the follow-up works pay attention to the abundance of paired dual-modal datasets [5, 26, 61, 65] for the cross-modal retrieval task. Recently, PointBind [15] and LanguageBind [82] collect the paired multi-modal datasets, which include more than three modalities. These datasets use language as the bridge to build the "Text-X" paired datasets. However, these datasets combine multi-modal data by language, which leads to a lack of flexibility in modality combinations. For example, in training on these datasets, the model can't achieve combinations of only vi-

sual modalities, e.g., (image, event, and touch). In light of this, we build the first dataset that consists of seven modalities and enables omni-bind for any of them.

3. The Proposed OmniBind

3.1. Problem Setting and Overview

Problem Setting: We aim to address the challenges of 1) modality mismatch between training and inference, and 2) data-scale imbalance among modalities. These challenges make it hardly possible for the previous methods, e.g., [18, 28] that only utilize a single modality during inference. As defined in Eq. 1, we consider a function $F(\cdot)$ with multi-modal encoders trained with data samples $\{M_1, \dots, M_N\}$ from a total number of N modalities, where $M_1 = \{x_1^{M_1}, \dots, x_k^{M_1}\}$ and k is the batch size. Denote the number of input modalities as n , and it may vary under the following conditions:

- 1) When $n = 1$, $F(\cdot)$ can provide predictions based on a single modality input during inference;
- 2) When $n > 1$, $F(\cdot)$ can provide predictions for the inputs with any combination of the N modalities.

$$f(\{M_1, \dots, M_N\}) = \begin{cases} F(M_i), i \in \{1, \dots, N\}, & n = 1 \\ F(Combine(\{M_1, \dots, M_n\})), & n > 1 \end{cases} \quad (1)$$

where $Combine(\cdot)$ selects any combination of all N modalities $\{M_1, \dots, M_n\}$. This setting requires $F(\cdot)$ to support adaptive fusion of any combination of input modalities at inference, ranging from 1 to n modalities. For example, if $F(\cdot)$ is to encode image (I), touch (T), and event (E) modalities, the possible inference inputs include: I, T, E, I+T, I+E, T+E, and all three combined.

Overview: An overview of OmniBind is depicted in Fig. 2. *The key insight* of our OmniBind is "Modalities Help Modalities", which involves teaching data-constrained, *a.k.a., student*, modalities (audio, point cloud, event, touch and thermal) to be aligned with the well-trained data-abundant, *a.k.a., teacher*, modalities (image and text). This subtly enables the adaptive fusion of any modalities to build a unified representation space for any combinations. Specifically, OmniBind incorporates two training stages: **I**) We introduce the Cross-modal Alignment Distillation (CAD) module (Sec. 3.2), which aligns the student modalities with the teacher modalities; **II**) We propose the Adaptive Fusion (AF) module (Sec. 3.3) to fuse modalities, thereby building a unified representation space for any modality combinations. Moreover, we compile and align data from existing datasets of seven modalities with the support of the LLM [42] and MLLM [73] to construct the modality-free dataset encompassing any modality combinations (Sec. 3.4) for training and inference.

3.2. Cross-modal Alignment Distillation (CAD)

In Stage I, our CAD module aims to address the data-scale imbalance problem between student and teacher modalities and effectively align the student modalities with teacher modalities through knowledge distillation (KD), as shown in Fig. 2. Specifically, we randomly sample one, *e.g.*, touch, from the five student modalities. The sampled modality is then aligned with the teacher modalities, *i.e.*, image and text. After this, another modality, *e.g.*, event, is randomly sampled from the remaining four student modalities, and aligned with the teacher modalities. This cross-modal distillation process is iterated for five times in total. The sampled student modality is aligned with the teacher modalities using the same optimization strategy. Take touch as an example, as shown in Fig. 2, its embeddings $E_t = \{E_{t_1}, \dots, E_{t_k}\}$ are extracted using a learnable touch encoder.

For the teacher modalities, initially, we freeze the image and text encoders which are pre-trained with large-scale data samples as teacher models. The image and text embeddings are extracted from the image $\{x_1^{img}, \dots, x_k^{img}\}$ and text $\{x_1^{txt}, \dots, x_k^{txt}\}$ input, $E_v = \{E_{v_1}, \dots, E_{v_k}\}$ and $E_l = \{E_{l_1}, \dots, E_{l_k}\}$ for distillation, respectively. Following [14, 37], we employ the extracted text embeddings as the supervisory signal for KD with contrastive learning:

$$\mathcal{L}_{in} = -\log \frac{\exp(E_{t_i} \cdot E_{l_i}^T / \tau)}{\exp(E_{t_i} \cdot E_{l_i}^T / \tau) + \sum_{j \neq i} (\exp(E_{t_i} \cdot E_{l_j}^T / \tau))}, \quad (2)$$

To effectively train the touch modality, we distill knowledge in two aspects: 1) the cross-correspondence between embeddings from the teacher and student modalities, and 2) the self-correspondence of the extracted embeddings from each modality. For the former, we first calculate the cross-correspondence D_t^r of the teacher modalities, *i.e.*, us-

ing text and image embeddings $E_v = \{E_{v_1}, \dots, E_{v_k}\}$ and $E_l = \{E_{l_1}, \dots, E_{l_k}\}$:

$$D_t^r = \{E_{l_1}, \dots, E_{l_k}\} \cdot \{E_{t_1}, \dots, E_{t_k}\}^T, \quad (3)$$

Then, we transfer the cross-modality knowledge D_t^r to touch modality using the *Kullback-Leibler* (KL) divergence loss:

$$\mathcal{L}_{cr} = \sum D_t^r \log \left(\frac{D_t^r}{\{E_{l_1}, \dots, E_{l_k}\} \cdot \{E_{t_1}, \dots, E_{t_k}\}^T} \right), \quad (4)$$

Afterwards, we calculate the self-correspondence of the image modality D_{img}^l and text modality D_{txt}^l via inner-product, and average D_{img}^l and D_{txt}^l to get D_t^l :

$$D_t^l = (D_{img}^l \cdot D_{img}^{lT} + D_{txt}^l \cdot D_{txt}^{lT}) / 2, \quad (5)$$

We then regard the averaged self-correspondence D_t^l as the intra-modality knowledge for the touch modality. The KL divergence is applied as the loss for the intra-modality knowledge transfer:

$$\mathcal{L}_{se} = \sum D_t^l \log \left(\frac{D_t^l}{\{E_{t_1}, \dots, E_{t_k}\} \cdot \{E_{t_1}, \dots, E_{t_k}\}^T} \right). \quad (6)$$

The overall loss consists of:

$$\mathcal{L}_{stage1} = \mathcal{L}_{in} + \mathcal{L}_{cr} + \mathcal{L}_{se}. \quad (7)$$

This is the CAD module for the randomly sampled modality, *i.e.*, touch, and the same CAD module is performed for the other four student modalities. The proposed CAD module effectively reinforces student modalities, *i.e.*, touch, to be aligned with the teacher modalities, *i.e.*, text, by cross-modality and intra-modality knowledge. This alleviates the data-scale imbalance problems and aligns all the student modalities to the teacher modalities, paving the way to learning a unified representation space for training stage II.

3.3. Adaptive Fusion (AF)

After achieving the alignment between all student and teacher modalities, the AF module in Stage II, is designed to build a unified representation space for any modality combinations. The detailed structure of the AF module is depicted in Fig. 3. Here, the parameters of all modalities' encoders are frozen, including the teacher and student modalities. Specifically, we first randomly sample any combinations from all the modalities as inputs for the AF module. For example, we sample image, audio, event, and touch as input for the AF module, as shown in Fig. 3 (b).

Then the label embeddings $E_s = \{E_{s_1}, \dots, E_{s_k}\}$ are extracted by passing all the label texts into the text encoder. The multi-modal embeddings, *i.e.*, E_v, E_a, E_e, E_t

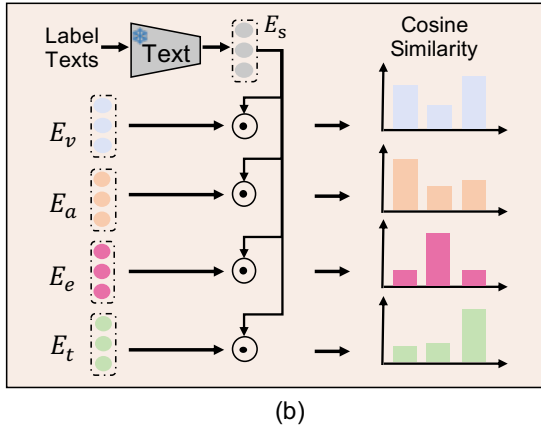
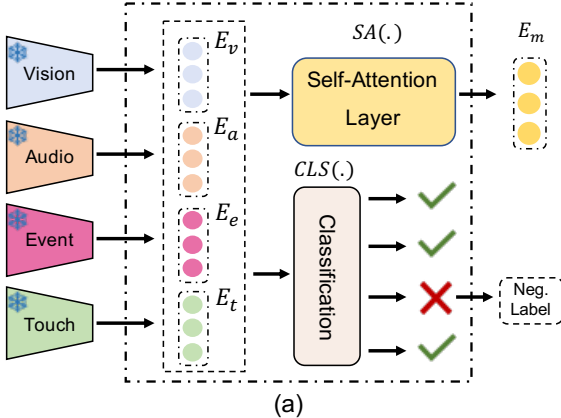


Figure 3. The Adaptive Fusion module. (a) The framework of our proposed AF module; (b) The details of the classification operation in the AF module.

in Fig. 3 (a), are obtained by passing any combination inputs to the corresponding multi-modal encoders. Afterwards, the multi-modal embeddings are passed to the ‘Classification’ operation $CLS(\cdot)$ in Fig. 3 (b), to find the output predictions for each modality. Concretely, we calculate the cosine similarity between all the label embeddings $E_s = \{E_{s_1}, \dots, E_{s_k}\}$ and the multi-modal embeddings E_v, E_a, E_e, E_t . For instance, the final prediction of input from vision modality is the corresponding label with the highest similarity score in $Sim(E_v, E_s)$. By doing so, we get the outputs for each modality in the combinations.

Subsequently, we use the real label as the benchmark to find the correct and incorrect predictions of all modalities. The incorrect predictions are used as negative supervision for improving the overall robustness of OmniBind. Actually, there is always at least one incorrect prediction among multi-modal inputs in experiments, and in case there is no incorrect prediction, AF module randomly picks one as a negative label for contrastive learning. Specifically, we fuse the multi-modal inputs using a self-attention layer $SA(\cdot)$ to obtain the final multi-modal embedding E_m for predictions:

$$E_m = \text{mean}(SA(E_v, \dots, E_t)), \quad (8)$$

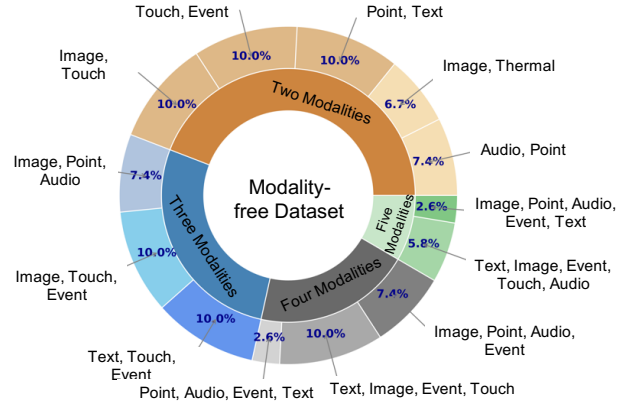


Figure 4. Overview of the modality-free dataset.

Dataset Details	Modality	Scale	#cls	Metric
ImageNet-1K (IN-1K) [9]	Image	1,280K	1,000	Acc
Caltech-101 (cal) [12]	Image	8K	101	Acc & Recall
ShapeNet-part (ShapeNet) [57]	Point Cloud	16K	16	Acc
ESC 5-folds (ESC) [45]	Audio	2K	50	Acc
Urban-Sound-8K (Urban-S) [48]	Audio	8K	10	Acc
LLVIP (LLVIP) [24]	Thermal	15K	2	Acc
N-ImageNet-1K (N-IN-1K) [27]	Event	1,280K	1,000	Acc
N-Caltech-101 (N-cal) [43]	Event	8K	101	Acc & Recall
Touch-and-Go (TouchGo) [65]	Touch	13.9K	20	Acc

Table 1. The details of source datasets in our modality-free dataset.

where $\text{mean}(\cdot)$ is the averaging function.

The contrastive loss for improving the overall robustness in Stage II can be expressed as:

$$\mathcal{L}_{stage2} = -\log \frac{\exp(E_m \cdot E_{pos}^T / \tau)}{\exp(E_m \cdot E_{pos}^T / \tau) + \sum_{j \neq i} (\exp(E_m \cdot E_{neg}^T / \tau))}, \quad (9)$$

where E_{pos} is the embeddings of [a photo of a "label"] and E_{neg} is the embeddings of [a photo of a "negative label"] extracted by the text encoder, as shown in Fig. 2. Overall, the AF module handles any modality combination inputs flexibly and exhibits robust performance across any modality combinations.

3.4. Modality-free Dataset

The goal of the proposed modality-free dataset is to address the mismatch problem between training and inference and also evaluate the effectiveness of our OmniBind. We construct the dataset consisting of any modality combinations for training and inference. We initially align the labels of multiple datasets, as enumerated in Tab. 1, powered by LLM [42]. Then we generate the descriptions for all the data samples via MLLM [73] and match the data samples with the same semantics of the descriptions. As depicted in Fig. 4, our dataset consists of 50,080 samples of modality combinations, with the most prevalent combinations being two modalities, accounting for 46%. The proportions for

Method	Combinations of Two Modalities				
	Point+Text	Image+Touch	Image+Thermal	Event+Touch	Point+Audio
ImageBind [14]+Mean	x	x	65.97	x	x
PointBind [15]+Mean	86.20	x	65.97	x	61.66
LanguageBind [82]+Mean	x	x	89.70	x	x
UniBind [37]+Mean	87.10	42.60	71.02	17.00	63.19
UniBind [37]+Unseen [75]	82.50	82.12	85.72	79.40	90.10
UniBind [37]+Linear	87.10	75.60	87.60	68.60	96.24
Ours	95.00	89.40	97.90	85.60	97.85
Δ	+7.90	+7.28	+10.30	+6.20	+1.61

Table 2. Results with the two-modality combinations. \times : not support.

Method	Three Modalities		Four Modalities		Five Modalities		Total
	C1	C2	C3	C4	C5	C6	
PointBind [15]+Mean	68.63	x	x	x	x	x	-
UniBind [37]+Mean	69.33	33.60	25.80	69.16	37.58	90.90	48.37
UniBind [37]+Unseen [75]	88.70	82.40	78.05	92.85	81.20	97.25	85.01
UniBind [37]+Linear	94.10	80.80	81.40	97.31	90.00	98.24	87.84
Ours	96.78	90.40	89.60	98.65	92.75	98.48	92.42
Δ	+2.68	+9.60	+8.20	+1.34	+2.75	+0.24	+4.05

Table 3. Results with the combinations (C) of three, four, and five modalities. Image: I, Audio: A, Point Cloud: P, Text: Te, Event: E, and Touch: T. C1: {I, A, P}; C2: {Te, E, T}; C3: {Te, E, T, I}; C4: {I, E, A, P}; C5: {Te, E, T, I, A}; C6: {I, P, A, E, Te}.

Model	ACC
VT CMC [65]	47.10
SSVTP [25]	47.60
VT CMC-all [65]	49.20
SSVTP-all [25]	43.80
UniTouch [64]	61.30
ViT-Lens [28]	63.11
Ours	67.45
Δ	+4.34

Table 4. Results on touch.

Model	ACC
RG-CNN [3]	65.70
EST [13]	81.70
DVS-ViT [53]	83.00
UniBind [37]	78.05
EventCLIP [58]	93.57
EventBind [80]	93.74
Ours	94.60
Δ	+0.86

Table 5. Results on event.

Model	ACC
ImageBind [14]	63.40
UniBind [37]	64.67
OpenCLIP [7]	82.20
LanguageBind [82]	88.91
Ours	92.60
Δ	+3.69

Table 6. Results on thermal.

three-modal, four-modal, and five-modal combinations are 15%, 16%, and 17%, respectively. *For more details of our dataset, please refer to the appendix.*

4. Experiments and Evaluation

4.1. Experimental Setup

Datasets: We compile our modality-free dataset from nine datasets. The details of these datasets are presented in Tab. 1. We show more details *in the appendix*. Additionally, we validate our OmniBind on three single-modality datasets and follow the benchmarks established by UniBind [37] and UniTouch [64]. Our performance on the student modalities is compared with existing baselines and state-of-the-art methods in Tab. 4, 5, and 6.

Backbone Models: We employ visual encoders from UniBind [37] for the image, point cloud, and audio modalities. For the event and thermal modalities, we enhance the existing UniBind encoders by adding an MLP (multi-layer perception) layer at the end. During training, we configure only the parameters of these MLP layers as learnable. Similarly, for the touch modality, we utilize UniBind’s image encoder augmented with an MLP layer at its end, setting only the MLP layer’s parameters as learnable.

Implementation Details: In the training process, our OmniBind is implemented in two stages. During CAD in Stage I, we freeze the parameters of the teacher modality encoders and set only the parameters of the student modality encoders as learnable. This strategy effectively facilitates the transfer of knowledge from the teacher to the student modalities. In

Stage II, we freeze the parameters of all the multi-modal encoders and only train the adaptive fusion module to achieve a unified representation space for any modality combinations. For comparison experiments, we employ baseline methods such as ImageBind [18], PointBind [15], LanguageBind [82], and UniBind [37]. As they cannot be used to accept any modality combination inputs, we add an **average fusion layer at the end** of them for fusing the modality embeddings. Additionally, we introduce two baseline models: UniBind+Linear, which incorporates a linear layer at the end of UniBind for recognizing multi-modal combinations; and UniBind+Unseen, which adds an unseen module from [75] to the end of UniBind. Furthermore, we compare our OmniBind with state-of-the-art methods for single modalities, such as UniTouch [64] and EventBind [80].

4.2. Results under Arbitrary Modality Combination Setting

We divide the comparison experiments into two categories according to the number of total modalities: two-modality combinations and more than three-modality combinations.

Two-modality Combinations. In Tab. 2, we present the experimental results for combinations of two modalities with our modality-free dataset. OmniBind demonstrates **robust performance** in recognizing combinations consisting of two modalities. Notably, OmniBind achieves **an average gain of 6.52% across all two-modality combinations**, including pairs such as (point, text), (image, touch), (image, thermal), (event, touch), and (point, audio). Specifically, OmniBind exhibits exceptional performance with combinations of student modalities, achieving a **6.20% gain** for the combinations of event and touch modalities. These robust results demonstrate the effectiveness of the CAD module in transferring knowledge from teacher modalities and crossing the data-scale gap between teacher and student modalities.

More than Three-modality Combinations. In Tab. 3, we illustrate OmniBind’s capability in processing combinations comprising more than three modalities. OmniBind achieves **an average improvement of +4.05%**. Particularly, OmniBind records more substantial gains with combinations involving more student modalities, such as a **9.60% improvement** with the combination of text, event, and touch modalities. This performance highlights the strengths of our approach in aligning student modalities and demonstrates its flexibility and effectiveness in recognizing and balancing combinations of more than three modalities.

4.3. Results under Single-modality Setting

Touch: As shown in Tab. 4, Compared to the state-of-the-art (SoTA) methods, OmniBind secures a significant improvement of +4.34% in the material recognition benchmark [65]. This gain highlights the superiority of OmniBind in single-modality recognition tasks.

Loss	Align Center	Touch	Event	Thermal
L_{in}	Text	61.79	85.10	87.10
$L_{in} + L_{cr}$		62.70	91.66	92.10
$L_{in} + L_{se}$		62.31	88.20	91.50
All		67.45	94.60	92.60
L_{in}	Image	48.68	78.90	58.72
$L_{in} + L_{cr}$		55.20	84.10	61.07
$L_{in} + L_{se}$		53.75	83.20	59.92
All		59.83	86.90	63.10

Table 7. Ablation of CAD’s losses.

Event: The quantitative results of OmniBind in the event modality is outlined in Tab. 4. OmniBind achieves SoTA performance on the N-Caltech dataset [43] while reducing **90%** of the learnable parameters compared with EventBind [80], the latest SoTA method in the event-based vision. **Thermal:** For the thermal modality, we compare the performance of OmniBind against experimental baselines. The recognition results on the LLVIP dataset [24] are reported, adhering to the benchmarks set by ImageBind [18]. OmniBind demonstrates strong performance, achieving a 3.69% gain on the thermal recognition benchmark [18].

5. Ablation Study

Effectiveness of the proposed loss functions. To evaluate the effectiveness of our proposed loss functions: L_{in} , L_{cr} , and L_{se} in CAD, we conduct ablation studies in the touch, event, and thermal modalities with image and text as align centers, respectively. The results, outlined in Tab. 7, demonstrate that all of these loss functions significantly improve the overall performance in three modalities. The cross-modal knowledge transferred by L_{cr} and the intra-modal knowledge transferred by L_{se} can be effective in improving performance and helping student modalities align to the teacher modalities’ representation space. Overall, the integration of all three proposed loss functions culminate in the highest performance, *i.e.*, **67.45% Acc for the touch modality, 94.60% Acc for the event modality, and 92.60% Acc for the thermal modality.** These results show the superiority of all loss functions in aligning student modalities with teacher modalities. We also show the ***t-SNE visualization*** of the representations of image, touch, and event modalities in Fig. 5 (a) and (b). Obviously, using our CAD makes the embeddings from different modalities become more clustered. The visualization results show that the proposed CAD can effectively align embeddings from different modalities in the high-level representation space.

Ablation of AF Module. As shown in Tab. 8, we show the efficiency of the $SA(\cdot)$ and the $CLS(\cdot)$ in the AF module. We conduct the experiments with any modality combinations, ranging from 2 to 5 modalities. Note that the

Method	2M	3M	4M	5M	Total
<i>Cat</i>	56.18	42.88	61.95	64.24	48.37
<i>CLS</i> (·)	92.54	91.03	92.29	93.45	91.07
<i>CLS</i> (·) + <i>SA</i> (·)	93.93	90.68	94.98	95.10	92.42

Table 8. Ablation study of the AF module. *Cat* means directly concatenating all the multi-modal embeddings for final predictions. *SA*(·) stands for the self-attention layer. (Modality: M)

Method	2M	3M	4M	5M	Total
Outer Product	22.50	28.91	41.20	44.82	33.67
Linear	83.03	87.36	92.65	94.14	87.84
<i>SA</i> (·) (Ours)	93.93	90.68	94.98	95.10	92.42

Table 9. Ablation study on the self-attention of AF module. Outer product and linear means we replace the *SA*(·) with outer product operation and a linear layer.

results in Tab. 8 are the average of all possible combinations. Both *CLS*(·) and *SA*(·) play positive roles in improving the overall performance, and using them simultaneously achieves the highest overall accuracy of 92.42%. Besides, we also assess the effectiveness of the *SA*(·) layer in Tab. 9. Evidently, replacing our *SA*(·) with an outer product or linear layer leads to significant performance drops. This indicates the superiority of the *SA*(·) in AF module.

Robustness of Adaptive Fusion Module. To assess the robustness of our AF module, we adopted the modality-noise setting proposed by Zhang et al.[75] to evaluate our approach. We randomly selected one input modality and introduced noise to it. As reported in Tab.11 in the appendix, OmniBind training with negative labels led to a **notable average improvement of +3.74%**. This enhancement underscores the crucial role of training with negative labels in boosting the robustness of OmniBind for modality combination recognition. Training with negative labels shows stronger performance gains with combinations of three modalities compared to those of four and five modalities, illustrating the advantages of our method in resisting a broader range of noise interference.

6. Discussion

Modality Combinations: We investigate the effectiveness of including more modalities in the combination on our dataset. As shown in Fig. 5 (c). OmniBind trained with three modalities exhibited the best performance, and training with two modalities showed significant improvement over training with a single modality. These results reveal the significance of our key idea "Modality Help Modality" and also show the importance of our Modality-free dataset.

Modality-free Dataset: In constructing the dataset, we employ coarse alignment at the label level and fine-grained alignment at the description level for assembling and col-

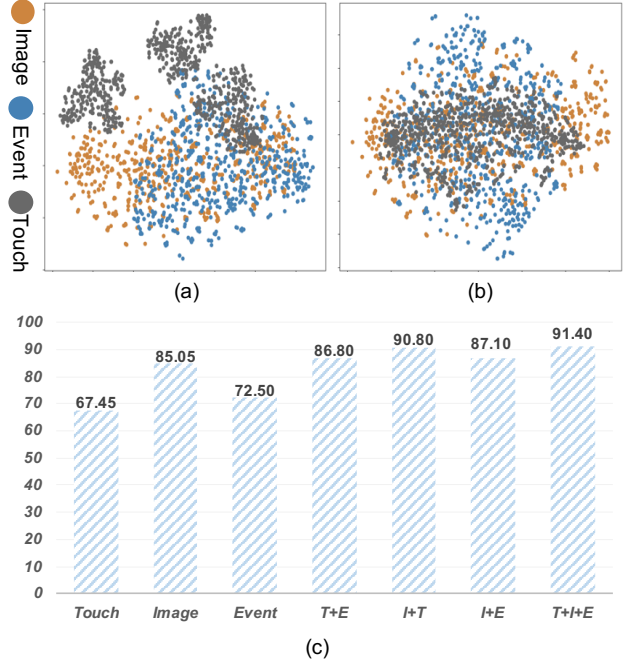


Figure 5. The t-SNE visualization (a) without CAD and (b) with CAD. (c): the ablation study of the modality numbers.

lecting the multi-modal combined data. The data obtained from this method are not perfectly aligned, but they do ensure semantic alignment. For recognition tasks, this approach is justifiable and aligns well with practical application scenarios where perfect alignment of multi-modal sensors cannot be guaranteed.

Broader Impacts: OmniBind enhances autonomous system adaptability, enabling robust performance in dynamic environments, which is beneficial for industrial automation and accessibility. However, its reliance on diverse modalities may increase complexity and resource demands.

7. Conclusion

In this paper, we proposed OmniBind, a universal multi-modal learning approach that crosses imbalance among multiple modalities and learns unified representations for any combination of modalities. **The key insight** of our OmniBind is "Modalities Help Modalities," which involves teaching data-constrained, *i.e.*, student, modalities (*e.g.*, touch and thermal) in alignment learning through well-trained data-abundant, *i.e.*, teacher, modalities (*e.g.*, image and texts) and further enables the flexible learning of unified representations for any combination of modalities.

Limitations and Future Works. There are still downstream applications of the free combinations of multiple modalities to be explored. In response, our future work will concentrate on applying OmniBind on more downstream multi-modal tasks.

References

- [1] Hangbo Bao, Wenhui Wang, Li Dong, Qiang Liu, Owais Khan Mohammed, Kriti Aggarwal, Subhojit Som, Songhao Piao, and Furu Wei. Vlmo: Unified vision-language pre-training with mixture-of-modality-experts. *Advances in Neural Information Processing Systems*, 35:32897–32912, 2022. [2](#)
- [2] Hangbo Bao, Wenhui Wang, Li Dong, Qiang Liu, Owais Khan Mohammed, Kriti Aggarwal, Subhojit Som, and Furu Wei. Vlmo: Unified vision-language pre-training with mixture-of-modality-experts. *arXiv preprint arXiv:2111.02358*, 2021. [2](#)
- [3] Yin Bi, Aaron Chadha, Alhabib Abbas, Eirina Bourtsoulatzé, and Yiannis Andreopoulos. Graph-based object classification for neuromorphic vision sensing. In *Proceedings of the IEEE/CVF international conference on computer vision*, pages 491–501, 2019. [6](#)
- [4] Runnan Chen, Youquan Liu, Lingdong Kong, Xinge Zhu, Yuexin Ma, Yikang Li, Yuenan Hou, Yu Qiao, and Wenping Wang. Clip2scene: Towards label-efficient 3d scene understanding by clip. In *Proceedings of the IEEE/CVF Conference on Computer Vision and Pattern Recognition*, pages 7020–7030, 2023. [2](#)
- [5] Xinlei Chen, Hao Fang, Tsung-Yi Lin, Ramakrishna Vedantam, Saurabh Gupta, Piotr Dollár, and C Lawrence Zitnick. Microsoft coco captions: Data collection and evaluation server. *arXiv preprint arXiv:1504.00325*, 2015. [3](#)
- [6] Yiting Cheng, Fangyun Wei, Jianmin Bao, Dong Chen, and Wenqiang Zhang. Cico: Domain-aware sign language retrieval via cross-lingual contrastive learning. In *Proceedings of the IEEE/CVF Conference on Computer Vision and Pattern Recognition*, pages 19016–19026, 2023. [2](#)
- [7] Mehdi Cherti, Romain Beaumont, Ross Wightman, Mitchell Wortsman, Gabriel Ilharco, Cade Gordon, Christoph Schuhmann, Ludwig Schmidt, and Jenia Jitsev. Reproducible scaling laws for contrastive language-image learning. In *Proceedings of the IEEE/CVF Conference on Computer Vision and Pattern Recognition*, pages 2818–2829, 2023. [6](#)
- [8] Ronald Clark, Sen Wang, Andrew Markham, Niki Trigoni, and Hongkai Wen. Vidloc: A deep spatio-temporal model for 6-dof video-clip relocalization. In *Proceedings of the IEEE conference on computer vision and pattern recognition*, pages 6856–6864, 2017. [2](#)
- [9] Jia Deng, Wei Dong, Richard Socher, Li-Jia Li, Kai Li, and Li Fei-Fei. Imagenet: A large-scale hierarchical image database. In *2009 IEEE conference on computer vision and pattern recognition*, pages 248–255. Ieee, 2009. [3](#), [5](#), [13](#)
- [10] Shengshun Duan, Qiongfeng Shi, and Jun Wu. Multimodal sensors and ml-based data fusion for advanced robots. *Advanced Intelligent Systems*, 4(12):2200213, 2022. [2](#)
- [11] Han Fang, Pengfei Xiong, Luhui Xu, and Yu Chen. Clip2video: Mastering video-text retrieval via image clip. *arXiv preprint arXiv:2106.11097*, 2021. [2](#)
- [12] Li Fei-Fei, Rob Fergus, and Pietro Perona. Learning generative visual models from few training examples: An incremental bayesian approach tested on 101 object categories. In *2004 conference on computer vision and pattern recognition workshop*, pages 178–178. IEEE, 2004. [5](#), [13](#)
- [13] Daniel Gehrig, Antonio Loquercio, Konstantinos G Derpanis, and Davide Scaramuzza. End-to-end learning of representations for asynchronous event-based data. In *Proceedings of the IEEE/CVF International Conference on Computer Vision*, pages 5633–5643, 2019. [6](#)
- [14] Rohit Girdhar, Alaaeldin El-Nouby, Zhuang Liu, Mannat Singh, Kalyan Vasudev Alwala, Armand Joulin, and Ishan Misra. Imagebind: One embedding space to bind them all. In *Proceedings of the IEEE/CVF Conference on Computer Vision and Pattern Recognition*, pages 15180–15190, 2023. [2](#), [4](#), [6](#), [13](#)
- [15] Ziyu Guo, Renrui Zhang, Xiangyang Zhu, Yiwen Tang, Xi-anzheng Ma, Jiaming Han, Kexin Chen, Peng Gao, Xi-anzhi Li, Hongsheng Li, et al. Point-bind & point-llm: Aligning point cloud with multi-modality for 3d understanding, generation, and instruction following. *arXiv preprint arXiv:2309.00615*, 2023. [2](#), [3](#), [6](#), [7](#)
- [16] Saurabh Gupta, Judy Hoffman, and Jitendra Malik. Cross modal distillation for supervision transfer. In *Proceedings of the IEEE conference on computer vision and pattern recognition*, pages 2827–2836, 2016. [3](#)
- [17] Andrey Guzhov, Federico Raue, Jörn Hees, and Andreas Dengel. Audioclip: Extending clip to image, text and audio. In *ICASSP 2022-2022 IEEE International Conference on Acoustics, Speech and Signal Processing (ICASSP)*, pages 976–980. IEEE, 2022. [2](#)
- [18] Jiaming Han, Renrui Zhang, Wenqi Shao, Peng Gao, Peng Xu, Han Xiao, Kaipeng Zhang, Chris Liu, Song Wen, Ziyu Guo, et al. Imagebind-llm: Multi-modality instruction tuning. *arXiv preprint arXiv:2309.03905*, 2023. [2](#), [3](#), [7](#)
- [19] Byeongho Heo, Jeessoo Kim, Sangdoon Yun, Hyojin Park, Nojun Kwak, and Jin Young Choi. A comprehensive overhaul of feature distillation. In *Proceedings of the IEEE International Conference on Computer Vision*, pages 1921–1930, 2019. [3](#)
- [20] Geoffrey Hinton, Oriol Vinyals, and Jeff Dean. Distilling the knowledge in a neural network. *arXiv preprint arXiv:1503.02531*, 2015. [3](#)
- [21] Tianyu Huang, Bowen Dong, Yunhan Yang, Xiaoshui Huang, Rynson WH Lau, Wanli Ouyang, and Wangmeng Zuo. Clip2point: Transfer clip to point cloud classification with image-depth pre-training. *arXiv preprint arXiv:2210.01055*, 2022. [2](#)
- [22] Soshi Iba, Christiaan JJ Paredis, and Pradeep K Khosla. Interactive multimodal robot programming. *The international journal of robotics research*, 24(1):83–104, 2005. [2](#)
- [23] Mahdi Ilami, Hosain Bagheri, Reza Ahmed, E Olga Skowronek, and Hamid Marvi. Materials, actuators, and sensors for soft bioinspired robots. *Advanced Materials*, 33(19):2003139, 2021. [2](#)
- [24] Xinyu Jia, Chuang Zhu, Minzhen Li, Wenqi Tang, and Wenli Zhou. Llvip: A visible-infrared paired dataset for low-light vision. In *Proceedings of the IEEE/CVF international conference on computer vision*, pages 3496–3504, 2021. [3](#), [5](#), [7](#), [13](#), [15](#)

- [25] Justin Kerr, Huang Huang, Albert Wilcox, Ryan Hoque, Jeffrey Ichnowski, Roberto Calandra, and Ken Goldberg. Self-supervised visuo-tactile pretraining to locate and follow garment features. *arXiv preprint arXiv:2209.13042*, 2022. 6
- [26] Chris Dongjoo Kim, Byeongchang Kim, Hyunmin Lee, and Gunhee Kim. Audiocaps: Generating captions for audios in the wild. In *Proceedings of the 2019 Conference of the North American Chapter of the Association for Computational Linguistics: Human Language Technologies, Volume 1 (Long and Short Papers)*, pages 119–132, 2019. 3
- [27] Junho Kim, Jaehyeok Bae, Gangin Park, Dongsu Zhang, and Young Min Kim. N-imagenet: Towards robust, fine-grained object recognition with event cameras. In *Proceedings of the IEEE/CVF international conference on computer vision*, pages 2146–2156, 2021. 5, 13
- [28] Weixian Lei, Yixiao Ge, Jianfeng Zhang, Dylan Sun, Kun Yi, Ying Shan, and Mike Zheng Shou. Vit-lens: Towards omnimodal representations. *arXiv preprint arXiv:2308.10185*, 2023. 2, 3, 6
- [29] Junnan Li, Dongxu Li, Silvio Savarese, and Steven Hoi. Blip-2: Bootstrapping language-image pre-training with frozen image encoders and large language models. *arXiv preprint arXiv:2301.12597*, 2023. 2
- [30] Junnan Li, Dongxu Li, Caiming Xiong, and Steven Hoi. Blip: Bootstrapping language-image pre-training for unified vision-language understanding and generation. In *International Conference on Machine Learning*, pages 12888–12900. PMLR, 2022. 2
- [31] Kang Li, Lequan Yu, Shujun Wang, and Pheng-Ann Heng. Towards cross-modality medical image segmentation with online mutual knowledge distillation. In *Proceedings of the AAAI Conference on Artificial Intelligence*, volume 34, pages 775–783, 2020. 3
- [32] Ziyi Lin, Shijie Geng, Renrui Zhang, Peng Gao, Gerard De Melo, Xiaogang Wang, Jifeng Dai, Yu Qiao, and Hongsheng Li. Frozen clip models are efficient video learners. In *European Conference on Computer Vision*, pages 388–404. Springer, 2022. 2
- [33] Ruiping Liu, Jiaming Zhang, Kunyu Peng, Yufan Chen, Ke Cao, Junwei Zheng, M Saquib Sarfraz, Kailun Yang, and Rainer Stiefelwagen. Fourier prompt tuning for modality-incomplete scene segmentation. *arXiv preprint arXiv:2401.16923*, 2024. 3
- [34] Zhenghao Liu, Chenyan Xiong, Yuanhuiyi Ly, Zhiyuan Liu, and Ge Yu. Universal vision-language dense retrieval: Learning a unified representation space for multi-modal retrieval. In *The Eleventh International Conference on Learning Representations*, 2022. 2
- [35] Huaishao Luo, Lei Ji, Ming Zhong, Yang Chen, Wen Lei, Nan Duan, and Tianrui Li. Clip4clip: An empirical study of clip for end to end video clip retrieval and captioning. *Neurocomputing*, 508:293–304, 2022. 2
- [36] Yuanhuiyi Lyu, Xu Zheng, and Lin Wang. Image anything: Towards reasoning-coherent and training-free multi-modal image generation. *arXiv preprint arXiv:2401.17664*, 2024. 3
- [37] Yuanhuiyi Lyu, Xu Zheng, Jiazhou Zhou, and Lin Wang. Unibind: Llm-augmented unified and balanced representation space to bind them all. *arXiv preprint arXiv:2403.12532*, 2024. 2, 4, 6, 7, 15
- [38] Tanvir Mahmud and Diana Marculescu. Ave-clip: Audioclip-based multi-window temporal transformer for audio visual event localization. In *Proceedings of the IEEE/CVF Winter Conference on Applications of Computer Vision*, pages 5158–5167, 2023. 2
- [39] Roxana Moreno and Richard Mayer. Interactive multimodal learning environments: Special issue on interactive learning environments: Contemporary issues and trends. *Educational psychology review*, 19:309–326, 2007. 1
- [40] Jishnu Mukhoti, Tsung-Yu Lin, Omid Poursaeed, Rui Wang, Ashish Shah, Philip HS Torr, and Ser-Nam Lim. Open vocabulary semantic segmentation with patch aligned contrastive learning. In *Proceedings of the IEEE/CVF Conference on Computer Vision and Pattern Recognition*, pages 19413–19423, 2023. 2
- [41] Jiquan Ngiam, Aditya Khosla, Mingyu Kim, Juhan Nam, Honglak Lee, and Andrew Y Ng. Multimodal deep learning. In *Proceedings of the 28th international conference on machine learning (ICML-11)*, pages 689–696, 2011. 1
- [42] OpenAI. Gpt-4 technical report, 2023. 4, 5, 13
- [43] Garrick Orchard, Ajinkya Jayawant, Gregory K Cohen, and Nitish Thakor. Converting static image datasets to spiking neuromorphic datasets using saccades. *Frontiers in neuroscience*, 9:437, 2015. 5, 7, 13, 15
- [44] Wonpyo Park, Dongju Kim, Yan Lu, and Minsu Cho. Relational knowledge distillation. In *Proceedings of the IEEE/CVF conference on computer vision and pattern recognition*, pages 3967–3976, 2019. 3
- [45] Karol J Piczak. Esc: Dataset for environmental sound classification. In *Proceedings of the 23rd ACM international conference on Multimedia*, pages 1015–1018, 2015. 3, 5, 13
- [46] Alec Radford, Jong Wook Kim, Chris Hallacy, Aditya Ramesh, Gabriel Goh, Sandhini Agarwal, Girish Sastry, Amanda Askell, Pamela Mishkin, Jack Clark, et al. Learning transferable visual models from natural language supervision. In *International conference on machine learning*, pages 8748–8763. PMLR, 2021. 2
- [47] Adriana Romero, Nicolas Ballas, Samira Ebrahimi Kahou, Antoine Chassang, Carlo Gatta, and Yoshua Bengio. Fitnets: Hints for thin deep nets. *arXiv preprint arXiv:1412.6550*, 2014. 3
- [48] Justin Salamon, Christopher Jacoby, and Juan Pablo Bello. A dataset and taxonomy for urban sound research. In *Proceedings of the 22nd ACM international conference on Multimedia*, pages 1041–1044, 2014. 5, 13
- [49] Hang Su, Wen Qi, Jiahao Chen, Chenguang Yang, Juan Sandoval, and Med Amine Laribi. Recent advancements in multimodal human–robot interaction. *Frontiers in Neuro-robotics*, 17:1084000, 2023. 2
- [50] Zineng Tang, Ziyi Yang, Chenguang Zhu, Michael Zeng, and Mohit Bansal. Any-to-any generation via composable diffusion. *Advances in Neural Information Processing Systems*, 36, 2024. 3
- [51] Lichen Wang, Jiayang Wu, Shao-Lun Huang, Lizhong Zheng, Xiangxiang Xu, Lin Zhang, and Junzhou Huang.

- An efficient approach to informative feature extraction from multimodal data. In *Proceedings of the AAAI Conference on Artificial Intelligence*, volume 33, pages 5281–5288, 2019. 3
- [52] Lin Wang and Kuk-Jin Yoon. Knowledge distillation and student-teacher learning for visual intelligence: A review and new outlooks. *IEEE Transactions on Pattern Analysis and Machine Intelligence*, 2021. 3
- [53] Zuowen Wang, Yuhuang Hu, and Shih-Chii Liu. Exploiting spatial sparsity for event cameras with visual transformers. In *2022 IEEE International Conference on Image Processing (ICIP)*, pages 411–415. IEEE, 2022. 6
- [54] Yixuan Wei, Yue Cao, Zheng Zhang, Houwen Peng, Zhu-liang Yao, Zhenda Xie, Han Hu, and Baining Guo. iclip: Bridging image classification and contrastive language-image pre-training for visual recognition. In *Proceedings of the IEEE/CVF Conference on Computer Vision and Pattern Recognition*, pages 2776–2786, 2023. 2
- [55] Ho-Hsiang Wu, Prem Seetharaman, Kundan Kumar, and Juan Pablo Bello. Wav2clip: Learning robust audio representations from clip. In *ICASSP 2022-2022 IEEE International Conference on Acoustics, Speech and Signal Processing (ICASSP)*, pages 4563–4567. IEEE, 2022. 2
- [56] Shengqiong Wu, Hao Fei, Leigang Qu, Wei Ji, and Tat-Seng Chua. Next-gpt: Any-to-any multimodal llm. *arXiv preprint arXiv:2309.05519*, 2023. 3
- [57] Zhirong Wu, Shuran Song, Aditya Khosla, Fisher Yu, Linguang Zhang, Xiaoou Tang, and Jianxiong Xiao. 3d shapenets: A deep representation for volumetric shapes. In *Proceedings of the IEEE conference on computer vision and pattern recognition*, pages 1912–1920, 2015. 3, 5, 13
- [58] Ziyi Wu, Xudong Liu, and Igor Gilitschenski. Eventclip: Adapting clip for event-based object recognition. *arXiv preprint arXiv:2306.06354*, 2023. 6
- [59] Zongwei Wu, Guillaume Allibert, Fabrice Meriaudeau, Chao Ma, and Cédric Demonceaux. Hidanet: Rgb-d salient object detection via hierarchical depth awareness. *IEEE Transactions on Image Processing*, 32:2160–2173, 2023. 2
- [60] Guodong Xu, Ziwei Liu, Xiaoxiao Li, and Chen Change Loy. Knowledge distillation meets self-supervision. In *European Conference on Computer Vision*, pages 588–604. Springer, 2020. 3
- [61] Jun Xu, Tao Mei, Ting Yao, and Yong Rui. Msr-vtt: A large video description dataset for bridging video and language. In *Proceedings of the IEEE conference on computer vision and pattern recognition*, pages 5288–5296, 2016. 3
- [62] Teng Xue, Weiming Wang, Jin Ma, Wenhai Liu, Zhenyu Pan, and Mingshuo Han. Progress and prospects of multimodal fusion methods in physical human–robot interaction: A review. *IEEE Sensors Journal*, 20(18):10355–10370, 2020. 2
- [63] Chuanguang Yang, Helong Zhou, Zhulin An, Xue Jiang, Yongjun Xu, and Qian Zhang. Cross-image relational knowledge distillation for semantic segmentation. In *Proceedings of the IEEE/CVF Conference on Computer Vision and Pattern Recognition*, pages 12319–12328, 2022. 3
- [64] Fengyu Yang, Chao Feng, Ziyang Chen, Hyoungeob Park, Daniel Wang, Yiming Dou, Ziyao Zeng, Xien Chen, Rit Gan-gopadhyay, Andrew Owens, et al. Binding touch to every-thing: Learning unified multimodal tactile representations. *arXiv preprint arXiv:2401.18084*, 2024. 2, 6, 7
- [65] Fengyu Yang, Chenyang Ma, Jiacheng Zhang, Jing Zhu, Wenzhen Yuan, and Andrew Owens. Touch and go: Learning from human-collected vision and touch. *arXiv preprint arXiv:2211.12498*, 2022. 3, 5, 6, 7, 13, 15
- [66] Li Yang, Yan Xu, Chunfeng Yuan, Wei Liu, Bing Li, and Weiming Hu. Improving visual grounding with visual-linguistic verification and iterative reasoning. In *Proceedings of the IEEE/CVF Conference on Computer Vision and Pattern Recognition*, pages 9499–9508, 2022. 2
- [67] Anbang Yao and Dawei Sun. Knowledge transfer via dense cross-layer mutual-distillation. *European Conference on Computer Vision*, 2020. 3
- [68] You Yu, Jiahong Li, Samuel A Solomon, Jihong Min, Jiaobing Tu, Wei Guo, Changhao Xu, Yu Song, and Wei Gao. All-printed soft human-machine interface for robotic physicochemical sensing. *Science robotics*, 7(67):eabn0495, 2022. 2
- [69] Jiaming Zhang, Huayao Liu, Kailun Yang, Xinxin Hu, Rui-ping Liu, and Rainer Stiefelhagen. Cmx: Cross-modal fusion for rgb-x semantic segmentation with transformers. *IEEE Transactions on Intelligent Transportation Systems*, 2023. 3
- [70] Pengchuan Zhang, Xiujun Li, Xiaowei Hu, Jianwei Yang, Lei Zhang, Lijuan Wang, Yejin Choi, and Jianfeng Gao. Vinvl: Revisiting visual representations in vision-language models. In *Proceedings of the IEEE/CVF conference on computer vision and pattern recognition*, pages 5579–5588, 2021. 2
- [71] Qiang Zhang, Changzhou Lai, Jianan Liu, Nianchang Huang, and Jungong Han. Fmcnet: Feature-level modality compensation for visible-infrared person re-identification. In *Proceedings of the IEEE/CVF conference on computer vision and pattern recognition*, pages 7349–7358, 2022. 3
- [72] Renrui Zhang, Ziyu Guo, Wei Zhang, Kunchang Li, Xupeng Miao, Bin Cui, Yu Qiao, Peng Gao, and Hongsheng Li. Pointclip: Point cloud understanding by clip. In *Proceedings of the IEEE/CVF Conference on Computer Vision and Pattern Recognition*, pages 8552–8562, 2022. 2
- [73] Renrui Zhang, Jiaming Han, Aojun Zhou, Xiangfei Hu, Shilin Yan, Pan Lu, Hongsheng Li, Peng Gao, and Yu Qiao. Llama-adapter: Efficient fine-tuning of language models with zero-init attention. *arXiv preprint arXiv:2303.16199*, 2023. 4, 5, 13
- [74] Yiyuan Zhang, Kaixiong Gong, Kaipeng Zhang, Hongsheng Li, Yu Qiao, Wanli Ouyang, and Xiangyu Yue. Meta-transformer: A unified framework for multimodal learning. *arXiv preprint arXiv:2307.10802*, 2023. 2
- [75] Yunhua Zhang, Hazel Doughty, and Cees Snoek. Learning unseen modality interaction. *Advances in Neural Information Processing Systems*, 36, 2024. 2, 3, 6, 7, 8
- [76] Haojie Zhao, Junsong Chen, Lijun Wang, and Huchuan Lu. Arkitrack: a new diverse dataset for tracking using mobile rgb-d data. In *Proceedings of the IEEE/CVF Conference on Computer Vision and Pattern Recognition*, pages 5126–5135, 2023. 2

- [77] Long Zhao, Xi Peng, Yuxiao Chen, Mubbasir Kapadia, and Dimitris N Metaxas. Knowledge as priors: Cross-modal knowledge generalization for datasets without superior knowledge. In *Proceedings of the IEEE/CVF Conference on Computer Vision and Pattern Recognition*, pages 6528–6537, 2020. [3](#)
- [78] Jiangbin Zheng, Yile Wang, Cheng Tan, Siyuan Li, Ge Wang, Jun Xia, Yidong Chen, and Stan Z Li. Cvt-slr: Contrastive visual-textual transformation for sign language recognition with variational alignment. In *Proceedings of the IEEE/CVF Conference on Computer Vision and Pattern Recognition*, pages 23141–23150, 2023. [2](#)
- [79] Xu Zheng and Lin Wang. Eventdance: Unsupervised source-free cross-modal adaptation for event-based object recognition. *arXiv preprint arXiv:2403.14082*, 2024. [3](#)
- [80] Jiazhou Zhou, Xu Zheng, Yuanhuiyi Lyu, and Lin Wang. E-clip: Towards label-efficient event-based open-world understanding by clip. *arXiv preprint arXiv:2308.03135*, 2023. [6](#), [7](#)
- [81] Luwei Zhou, Hamid Palangi, Lei Zhang, Houdong Hu, Jason Corso, and Jianfeng Gao. Unified vision-language pre-training for image captioning and vqa. In *Proceedings of the AAAI conference on artificial intelligence*, volume 34, pages 13041–13049, 2020. [2](#)
- [82] Bin Zhu, Bin Lin, Munan Ning, Yang Yan, Jiaxi Cui, HongFa Wang, Yatian Pang, Wenhao Jiang, Junwu Zhang, Zongwei Li, et al. Languagebind: Extending video-language pretraining to n-modality by language-based semantic alignment. *arXiv preprint arXiv:2310.01852*, 2023. [2](#), [3](#), [6](#), [7](#)
- [83] Xiangyang Zhu, Renrui Zhang, Bowei He, Ziyao Zeng, Shanghang Zhang, and Peng Gao. Pointclip v2: Adapting clip for powerful 3d open-world learning. *arXiv preprint arXiv:2211.11682*, 2022. [2](#)

Appendix

A. More Details of Datasets

A.1. More Details of Source Datasets

ImageNet-1K (IN-1K) [9]. This dataset is a fundamental image repository designed for recognition tasks, encompassing over 1,000 categories. It is utilized for both training and evaluation purposes. In the zero-shot setting, we assess both baseline models and our proposed method on the test set without prior training, employing accuracy as the metric for evaluation.

Caltech-101 (Cal) [12]. The Caltech-101 dataset is an established benchmark in computer vision, specifically designed for object recognition tasks. It comprises images from 101 diverse object categories, reflecting a variety of real-world scenes. In this study, we use the dataset for model evaluation in object recognition and extend its use to cross-modal retrieval tasks involving Caltech-101 and N-Caltech-101. Accuracy is the metric for recognition.

ShapeNet-part (ShapeNet) [57]. ShapeNet-part is a key benchmark dataset widely used for 3D segmentation tasks. In this work, we frame the evaluation on ShapeNet-part as a recognition task. The dataset includes 16 categories of 3D objects, with accuracy as the chosen evaluation metric.

ESC 5-folds (ESC) [45]. This dataset includes 2,000 audio clips, each lasting five seconds and classified into 50 distinct categories. In the zero-shot setting, we utilize the entire dataset to assess both baseline models and our proposed method. For fine-tuning, models are trained on the designated training set and evaluated on the test set, using accuracy as the evaluation metric.

Urban-Sound-8K (Urban-S) [48]. The UrbanSound8K dataset is a widely used collection of audio data designed for research in the field of urban sound recognition. Urban-Sound8K consists of 8,732 audio clips, each lasting 4 seconds. These clips are extracted from longer field recordings and are labeled with specific sound classes. The dataset is annotated with 10 sound classes and we evaluate models on the test set with accuracy metric.

LLVIP (LLVIP) [24]. The LLVIP dataset features RGB and Thermal image pairs. Following the approach in ImageBind[14], we use it for binary classification tasks, extracting pedestrian and random bounding boxes to create a balanced dataset of 15,809 boxes. Top-1 accuracy is the evaluation metric.

N-ImageNet-1K (N-IN-1K) [27]. N-ImageNet-1K encompasses paired event data derived from the ImageNet-1K [9] dataset. The evaluation focuses on assessing the event recognition capabilities of models within this dataset. Accuracy is employed as the metric for this evaluation.

N-Caltech-101 (N-Cal) [43]. N-Caltech-101 includes paired event data related to the Caltech-101 dataset. This

dataset is used for event recognition and both event-to-image and image-to-event retrieval tasks. Accuracy is the respective metric for recognition tasks.

Touch-and-Go (TouchGo) [65]. Touch-and-Go is a dataset with paired visual and tactile data. This dataset is collected from probe objects in natural environments using tactile sensors, while simultaneously recording egocentric video. The metric for the recognition task is top-1 accuracy.

A.2. More Details of Modality-free Dataset

We constructed a modality-free dataset from a range of source datasets, including ImageNet-1K, Caltech-101, ShapeNet, ESC-50, Urban-Sound-8K, LLVIP, N-ImageNet-1K, N-Caltech-101, and Touch-and-Go. As illustrated in Fig. 6, we initially aligned the labels across seven modalities using the LLM (ChatGPT-4[42]) to ensure semantic correspondence between the categories. Subsequently, we utilized the MLLM (LLaMA-Adapter[73]) to generate descriptive texts for various visual modalities, thereby facilitating sample-level matching through similarity calculations between text descriptions and visual data. The process of generating these descriptions is detailed in Fig. 8.

Specifically, we derive audio and point cloud sets with matching semantics by analyzing and aligning the labels of both datasets using language modeling techniques. This alignment ensures that labels share identical meanings across modalities. Subsequently, as depicted in Fig. 8, we employ the LLaMA-Adapter to generate descriptive texts for both the audio and point cloud data. We then establish correspondence between the audio files and point clouds based on the semantic content of their descriptions, calculating cosine similarity between the text embeddings of descriptions from the audio and point cloud datasets.

Lastly, we present the data distribution of each label as a word cloud in Fig. 7. It demonstrates the equalization of our dataset among categories.

B. More Details of Our Proposed OmniBind

We show more details of our proposed OmniBind in the demo code. We show the training code of knowledge-distilled alignment learning in code *DemoKDAL.py*, and we show the code of our OmniBind model in code *OmniBind.py*. We provide our project code and some cases of modality-free datasets in the *supplementary material*.

```
def train(args, model, train_dataloader, device):
    real_batch_size = args.train_batch_size *
        args.gradient_steps
    t_total = train_dataloader.dataset.__len__()
    //
    real_batch_size * args.num_train_epochs
    param_optimizer = list(model.named_parameters
        ())
    optimizer_grouped_parameters = [
```



```

        s_logic = v_embeddings @ t_embeddings
    .t()
    kl_loss = kldivloss(s_logic, t_logic)
    self_t_logic = t_embeddings @
t_embeddings.t()
    self_s_logic = v_embeddings @
v_embeddings.t()
    self_kl_loss = kldivloss(self_s_logic
, self_t_logic)
    loss = (cl_loss+kl_loss*100+
self_kl_loss*100)/3
    if args.gradient_accumulation_steps >
1:
        loss = loss / args.
gradient_accumulation_steps
        loss.backward()
        tr_loss += loss.item()
        if (step + 1) % args.
gradient_accumulation_steps == 0:
            global_step += 1
            torch.nn.utils.clip_grad_norm_(
model.parameters(), args.
max_grad_norm)
            writer.add_scalar(tag="cl_loss",
scalar_value=
tr_loss / global_step,
global_step=step+epoch_steps*
epoch)
            optimizer.step()
            scheduler.step()
            model.zero_grad()
            if global_step % args.eval_steps
== 0:
                logger.info('Start eval!')
                acc = evaluate()
                logger.info('Dev acc: {0}'.
format(acc))
                if acc >= best_acc:
                    best_acc = acc
                    torch.save(
                        model.state_dict(),
                        args.ckpt_dir
                    )
            writer.close()
            torch.save(model.state_dict(), args.ckpt_dir)

```

DemoKDAL.py

```

class OmniBind(nn.Module):
    def __init__(self, args):
        super(OmniBind, self).__init__()
        self.modality = args.modality
        self.backbone = UniBind.load(args.
pre_train_weights)
        for param in self.backbone.parameters():
            param.requires_grad_(False)
        self.fuse_adapter = Adapter(args.dim,
args.head_num)
    def forward(self, inputs):
        embeddings = self.backbone(inputs)
        fuse_embedding = self.fuse_adapter(
embeddings).mean(dim=1)
        fuse_embedding /= fuse_embedding.norm(dim
=-1, keepdim=True)
        return fuse_embedding

```

OmniBind.py

Modality	Dataset	batch size	lr	total epochs
Touch	Touch-and-Go [65]	512	5e-4	20
Thermal	LLVIP [24]	256	1e-3	20
Event	N-Caltech-101 [43]	128	5e-4	20
All	Modality-free	512	1e-3	10

Table 10. The hyperparameters of experiments with the proposed OmniBind.

Method	Combination 7	Combination 8	Total
UniBind [37]	33.60	80.90	48.37
UniBind-linear [37]	87.20	90.40	87.48
Ours	93.40	99.24	92.42
Δ	+6.20	+8.84	+4.94

Table 11. The additional experiment results on the modality-free dataset. Combination 7: image, touch, and event; Combination 8: point cloud, audio, event, and text.

Method	Three Modalities	Four Modalities	Five Modalities	Total
UniBind [37]+mean	17.23	61.82	64.25	46.81
UniBind [37]+linear	60.22	91.98	93.92	80.39
Ours w/o Neg. Label	70.74	90.68	93.27	83.20
Ours	78.20	93.36	94.75	86.94
Δ	+7.46	+2.68	+1.48	+3.74

Table 12. The ablation study for exploring the robustness of OmniBind.

C. Training Setup

Our experiments were done on 80GB A100 GPUs, and we detail the hyperparameters used for training for stages 1 and 2 reported in Tab. 10.

D. Additional Results

We showcase more results with the combinations of three modalities and four modalities in Tab. 11. For these additional combination inputs, our OmniBind achieves *an average performance gain of 4.94%*.

E. Additional Ablation studies

To further analyze the robustness of our OmniBind framework, we conduct ablation studies by introducing noise into specific modalities to assess the model’s robustness to noise across different modalities. As depicted in Tab. 13, the performance significantly decreases when noise is added to the teacher modalities (text and image). In contrast, OmniBind exhibits a strong resilience to noise in the event and touch modalities. This observation suggests that the primary modality continues to play a dominant role in the interaction of multiple modalities.

Noise Modality	Three Modalities		Four Modalities		Five Modalities	
	Combination 1	Combination 2	Combination 3	Combination 4	Combination 5	Combination 6
Null	96.78	90.40	89.60	98.65	92.75	98.48
text	96.78	6.8	8.9	98.65	37.58	52.27
Δ	-	-83.60	-80.70	-	-55.17	-46.21
Event	96.78	77.00	80.8	95.42	87.93	93.25
Δ	-	-13.40	-8.8	-3.23	-4.82	-5.23
Touch	96.78	75.40	79.01	98.65	85.90	98.48
Δ	-	-15.00	-10.59	-	-6.85	-

Table 13. Effect of different noise modality on the performance. Combination 1: image, audio, and point cloud; Combination 2: text, event, and touch; Combination 3: text, event, touch, and image; Combination 4: image, event, audio, and point cloud; Combination 5: text, event, touch, image, and audio; Combination 6: image, point cloud, audio, event, and text